

# Solid solution range of boron and properties of the perovskite-type $\text{NdRh}_3\text{B}$

Shigeru OKADA<sup>\*1,†</sup>, Kunio KUDOU<sup>\*2</sup>, Kiyokata IIZUMI<sup>\*3</sup>,  
Kazuo NAKAJIMA<sup>\*4</sup>, Toetsu SHISHIDO<sup>\*5</sup>

**Abstract:** Polycrystalline samples of  $\text{NdRh}_3\text{B}_x$  have been synthesized by arc melting technique. The crystal structure of  $\text{NdRh}_3\text{B}_x$  is the perovskite-type cubic system (space group  $Pm\bar{3}m$ ) for nominal boron concentration in the range of  $0.706 \leq x \leq 1.000$  (15–20 mol. % B). The lattice parameter  $a$  varies linearly from 0.41749(7) nm ( $x = 0.706$ ) to 0.42136(6) nm ( $x = 1.000$ ). Thermogravimetric analysis indicates that the oxidation onset temperature for  $\text{NdRh}_3\text{B}_{1.000}$  is 663 K. The weight gain of the sample by heating in air up to 1473 K is 10.00% for  $\text{NdRh}_3\text{B}_{1.000}$ , and oxidized products are Rh and  $\text{NdBO}_3$ . The micro-Vickers hardness is  $4.9 \pm 0.05$  GPa for  $\text{NdRh}_3\text{B}_{1.000}$ .  $\text{NdRh}_3\text{B}_{1.000}$  shows a metallic temperature dependence of the resistivity down to 0.5 K. Magnetic susceptibilities for  $\text{NdRh}_3\text{B}_{1.000}$  show Curie-like paramagnetic temperature dependence due to  $\text{Nd}^{3+}$  moments. No trace of magnetic phase transitions and superconductivity is found.

**Keywords:**  $\text{NdRh}_3\text{B}$ ; Microhardness; Oxidation resistance in air; Electric property; Magnetic property

## 1. Introduction

The rare earth element (RE)-platinum group element-boron systems have received considerable attention from many researchers in the fields of crystallography, magnetism, superconductivity, heavy-electron behavior and valence fluctuations. Particularly, the discovery of the  $\text{ErRh}_4\text{B}_4$  compound, which is a re-entrant superconductor, has drawn much attention to these ternary systems [1,2]. We have previously prepared single crystals of several compounds by molten metal flux method, using Cu as a flux. They are  $\text{ErRh}_3\text{B}$  (cubic system, space group:  $Pm\bar{3}m$ ,  $a = 0.4146$  nm),  $\text{ErRh}_3\text{B}_2$  (base-centered monoclinic system,  $\text{ErIr}_3\text{B}_2$  type, space group:  $C2/m$ ,  $a = 0.5355(1)$  nm,  $b = 0.9282(1)$  nm,  $c = 0.3102(1)$  nm,  $\beta = 90.89(3)^\circ$ ) and  $\text{ErRh}_4\text{B}_4$  (simple tetragonal system, space group:  $P4_2/nmc$ ,  $a = 0.5304(1)$  nm,  $c = 0.7395(2)$  nm). The physical and

chemical properties of these crystals have been reported [3,4].

Many studies of perovskite-type oxides have been performed due to the interesting features in the superconducting transition, the insulator-metallic transition, ion conduction characteristics, dielectric properties, and ferroelasticity. On the other hand, there have been few studies on non-oxide perovskite-type compounds [5,6].

We have previously prepared  $\text{RERh}_3\text{B}$  (RE = La, Gd and Lu) by arc-melting synthetic method [7,8], where La, Gd and Lu are the first, middle and last elements of the lanthanoids, in which RE is positioned at the eight corners of the cube, Rh is face-centered and B is body-centered. The B-deficient compounds,  $\text{RERh}_3\text{B}_x$ , can also be obtained. The B content variation induces changes in the electromagnetic properties, hardness and chemical resistance against oxidation in air at high temperature.

In this study, we focused on the less than half element of Nd (atomic number 60) in the lanthanoids. We synthesized the perovskite-type compound  $\text{NdRh}_3\text{B}_x$ . The solid solution range of boron in the  $\text{NdRh}_3\text{B}_x$  is clarified by powder X-ray diffraction (XRD) analysis, and the variation of the lattice constant of the sample is investigated as a function of the boron concentration  $x$ . Vickers microhardness ( $H_V$ ) and thermogravimetric and differential thermal analysis (TG-DTA) measurements were performed on the samples. The temperature dependence of the electrical resistance and magnetization was studied for the samples.

## 2. Experimental

### 2.1 Sample preparation

Polycrystalline samples of  $\text{NdRh}_3\text{B}_x$  were synthesized by the arc melting method using 99.9% pure Nd, Rh and B as

<sup>\*1</sup> 工学部都市システム工学科, 教授, 工学博士  
Department of Civil and Environmental Engineering,  
Faculty of Engineering, Professor, Dr. of Engineering

<sup>†</sup> Corresponding author. Tel/fax: +81-3-5481-3292, E-mail  
address: sokada@kokushikan.ac.jp (S. Okada).

<sup>\*2</sup> 神奈川大学, 工学部機械工学科, 助教授, 博士 (工学)  
Department of Mechanical Engineering, Faculty of Engineering,  
Kanagawa University, Associate Professor, Dr. of Engineering

<sup>\*3</sup> 東京工芸大学, 工学部ナノ化学科, 助教授, 博士 (工学)  
Faculty of Engineering, Tokyo Polytechnic University, Associate Professor,  
Dr. of Engineering

<sup>\*4</sup> 東北大学金属材料研究所, 教授, 工学博士  
Institute for Materials Research, Tohoku University,  
Professor, Dr. of Engineering

<sup>\*5</sup> 東北大学金属材料研究所, 助教授, 工学博士  
Institute for Materials Research, Tohoku University, Associate Professor,  
Dr. of Engineering

raw materials. These were weighed in the atomic ratio 1 : 3 :  $x$ , where  $x=1.000$  (20 mol.% B), 0.848 (17.5 mol.% B), 0.706 (15 mol.% B), 0.444 (10 mol.% B), 0.210 (5 mol.% B), and 0 (0 mol.% B). The mixture of the starting materials, about 2 g for each sample, was placed in a water-cooled copper hearth in a reaction chamber. Argon was used as a protective atmosphere. The pressure inside the chamber was  $\sim 1$  atm. A small amount of residual oxygen in argon was eliminated by fusing a button of titanium as a reducing agent. The starting materials were then melted for 3 min by an argon arc plasma flame with DC power source at 20 V and 100 A. The samples were then turned over and melted three times under the same conditions. Finally, synthesized samples were wrapped in tantalum foil and annealed at 1573 K for 20 h under vacuum to ensure homogeneity.

## 2.2 Characterization

For chemical analysis, the samples were fused using  $\text{NaHSO}_4$  as a flux reagent, then the obtained material was dissolved into HCl. The chemical composition of each solution was analyzed by the induction coupled plasma atomic emission spectrometry (ICP-AES) method, using Zn as internal standard. Crystal structure characterization of the samples was performed by XRD. The micro-Vickers hardness for the samples was measured at room temperature. A load of 100 g was applied for 15 s and 10 impressions were recorded for each sample. The obtained values were averaged and the experimental error was estimated. Thermogravimetric analysis and differential thermal analysis were performed between room temperature and 1473 K to study the oxidation resistance of the samples in air. A sample was heated at a rate of 10 K/min up to 1473 K. The oxidation products were analyzed by powder X-ray diffractometry. The electrical resistivity of the samples was measured by means of a DC four probe method from 0.5 K to room temperature. The magnetic susceptibility measurements were performed in a field of 5000 Oe using a commercial SQUID magnetometer (Quantum Design Inc., MPMS-5) from 5 K to room temperature.

## 3. Results and discussion

### 3.1 Appearance and chemical composition of synthesized material

Since the boiling points of Nd, Rh and B are high at 3373, 4233 and 2823 K, respectively, evaporation can be neglected [9]. Accordingly, we judge that the arc melting method is suitable for the synthesis of  $\text{NdRh}_3\text{B}_x$ . Samples of  $\text{NdRh}_3\text{B}_x$  obtained by varying the B content  $x$  were all silver in color and exhibited a metallic luster. The result of chemical analysis shows that the chemical compositions before and after synthesis are almost the same. In addition, contamination from the electrode (tungsten) and hearth (copper) could be disregarded in this study.

### 3.2 Relationship between the nonstoichiometry of B and the lattice constant of $\text{NdRh}_3\text{B}_x$ samples

The crystal structure analysis on  $\text{NdRh}_3\text{B}_x$  samples with a B content of  $x=1.000$  by powder XRD reveals that it is a

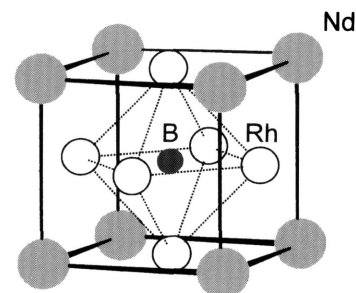


Fig. 1. Arrangement of atoms in the perovskite-type  $\text{NdRh}_3\text{B}$ . Large gray, large open and small black circles represent Nd, Rh and B atoms, respectively.

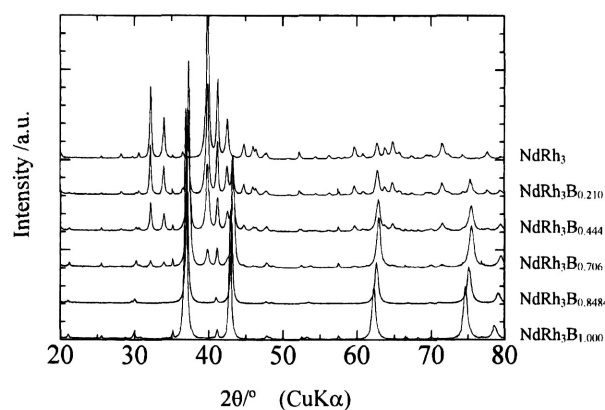


Fig. 2. Powder XRD profiles for  $\text{NdRh}_3\text{B}_x$  with  $x=1.000$ ,  $x=0.8484$ ,  $x=0.706$ ,  $x=0.444$ ,  $x=0.210$  and  $x=0$ . These are nominal compositions. In the cases of  $x=0.706$ ,  $x=0.444$  and  $x=0.210$ , a mixture phase of  $\text{NdRh}_3\text{B}_x$  and  $\text{NdRh}_3$  is formed.

perovskite-type compound (space group:  $Pm\bar{3}m$ ) in which Nd is positioned at the eight corners of the cube, Rh is face-centered and B is body-centered (Fig. 1). By varying  $x$ , the nonstoichiometry of B and the resulting change of the crystal structure were studied. Fig. 2 shows changes of the powder XRD patterns when  $x$  is varied. With decreasing  $x$ , the XRD peaks of the perovskite-type phase are shifted to higher angles. In the cases of  $x=0.706$ , 0.444 and 0.210, two phases of  $\text{NdRh}_3\text{B}_x$  and  $\text{NdRh}_3$  are observed.

Fig. 3 shows the relationship between  $x$  and the lattice constant of  $\text{NdRh}_3\text{B}_x$ . The lattice constant changes almost linearly with  $x$ , varying from  $a=0.41749(7)$  nm ( $x=0.706$ ) to  $a=0.42136(6)$  nm ( $x=1.000$ ). Table 1 shows the lattice parameters of the  $\text{NdRh}_3\text{B}_x$ . Accordingly,  $\text{NdRh}_3\text{B}_x$  exists in a nonstoichiometric range of  $0.706 \leq x \leq 1.000$ . Meanwhile, according to our experimental results for  $\text{LaRh}_3\text{B}_x$ , the perovskite-type compound does not have B-nonstoichiometry, which indicates that  $x=1$ . In the case of  $\text{GdRh}_3\text{B}_x$  and  $\text{LuRh}_3\text{B}_x$ , B-nonstoichiometry ranges within  $0.55 \leq x \leq 1.00$  and  $0.30 \leq x \leq 1.00$ , respectively. The aforementioned results are listed in Table 2. As shown in Table 2, B exhibits no nonstoichiometry in the case of RE = La.

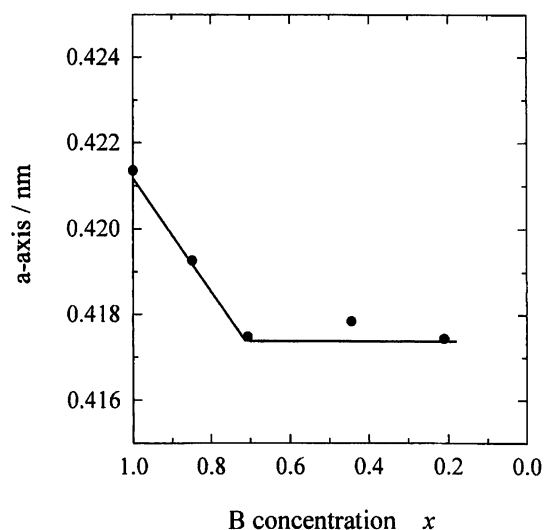


Fig. 3. The variation of lattice constant  $a$  as a function of boron concentration  $x$  in  $\text{NdRh}_3\text{B}_x$ .

Table 1 Lattice parameter of the  $\text{NdRh}_3\text{B}_x$

Sample (at. % of boron)	Lattice parameter $a$ , nm	Error nm
$\text{NdRh}_3\text{B}_{1.000}(20)$	0.41236	0.00006
$\text{NdRh}_3\text{B}_{0.848}(17.5)$	0.41927	0.00008
$\text{NdRh}_3\text{B}_{0.706}(15)$	0.41749	0.00007
$\text{NdRh}_3\text{B}_{0.444}(10)$	0.4179	0.0001
$\text{NdRh}_3\text{B}_{0.210}(5)$	0.4175	0.0001

Table 2 Boron nonstoichiometry in the  $\text{RERh}_3\text{B}_x$  (RE = La, Nd, Gd, Lu)

$\text{RERh}_3\text{B}_x$ RE	Boron nonstoichiometry range of $x$	Reference
La	$x = 1$	[8]
Nd	$0.71 \leq x \leq 1$	This study
Gd	$0.55 \leq x \leq 1$	[7]
Lu	$0.30 \leq x \leq 1$	[8]

La has the largest atomic radius among all the RE elements, while B gradually became nonstoichiometric as the atomic radius is decreased in the order of Nd, Gd and Lu. Electro negativity of the RE elements changes from 1.1 (La) to 1.2 (Lu). Electronegativity of the RE atoms seems to also affect boron nonstoichiometry of the  $\text{RERh}_3\text{B}_x$ .

### 3.3 Relationship between B content and hardness in $\text{NdRh}_3\text{B}_x$

We studied the hardness of  $\text{NdRh}_3\text{B}_x$ , which reflects the nature of the chemical bonding. Table 3 shows that the microhardness of the compound is  $4.3 \pm 0.2$  and  $4.9 \pm 0.05$  GPa when  $x = 0.848$  and  $1.000$ , respectively. In a previous study, as shown in Table 3, the value of microhardness for an Rh–B binary system increased with boron content of

Table 3 Vickers hardness of the  $\text{NdRh}_3\text{B}_x$

Sample (at. % of boron)	Hardness, GPa
$\text{NdRh}_3\text{B}_{1.000}(20)^a$	$4.9 \pm 0.05$
$\text{NdRh}_3\text{B}_{0.848}(17.5)^a$	$4.3 \pm 0.2$
$\text{RhB}(50)^b$	12.1
$\text{Rh}_7\text{B}_3(30)^b$	7.8

<sup>a</sup> Cubic system.

<sup>b</sup> Hexagonal system.

Table 4 Vickers hardness of the  $\text{RERh}_3\text{B}_{1.000}$

Sample $\text{RERh}_3\text{B}_{1.000}$ RE	Hardness GPa	Atomic radius of RE (nm)	Density $\text{g}/\text{cm}^3$	Reference
La	$4.2 \pm 0.1$	0.188	9.91	[8]
Nd	$4.9 \pm 0.05$	0.182	10.30	This study
Gd	$6.8 \pm 0.1$	0.180	10.82	[7]
Lu	$7.7 \pm 0.5$	0.174	11.69	[8]

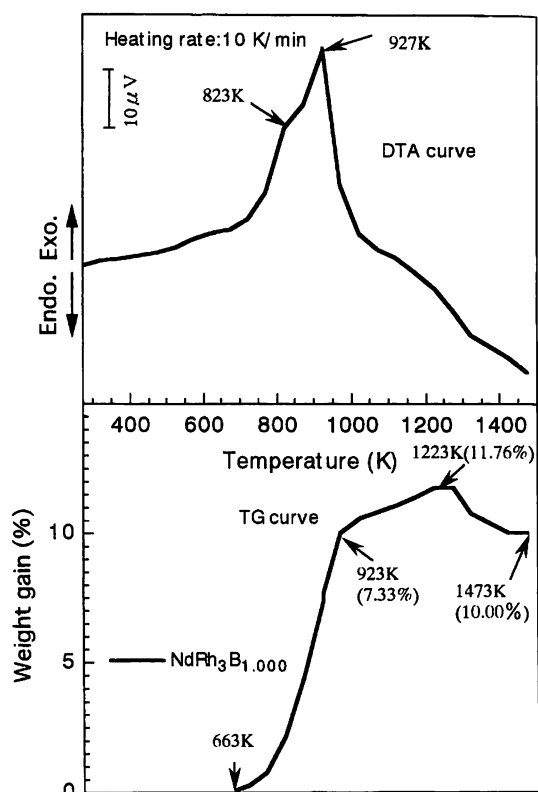
the compound [10]. This tendency of binary borides is essentially in agreement with our data on ternary borides. We then focused on only stoichiometric  $\text{RERh}_3\text{B}_{1.000}$ . The hardness in the series of RE = La, Nd, Gd and Lu is listed in Table 4. Hardness increases with decreasing atomic size of the RE in  $\text{RERh}_3\text{B}_{1.000}$ , it became greater with increasing density of itself. In all cases of RE = La, Nd Gd and Lu, hardness of the compound decreases with decreasing the boron content  $x$  in  $\text{RERh}_3\text{B}_x$ . In  $\text{GdRh}_3\text{B}_x$ , for example, boron nonstoichiometry ranges between  $0.55 \leq x \leq 1$  and hardness changes from  $4.0 \pm 0.1$  to  $6.8 \pm 0.1$  GPa, respectively.

### 3.4 Resistance to oxidation of $\text{NdRh}_3\text{B}_{1.000}$

We studied how the resistance to oxidation in air, which reflects the nature of the chemical bonds of the compound, varied with the B content. Samples were heated up to 1473 K in air and subjected to thermogravimetric and differential thermal analyses (TG–DTA). As shown in Fig. 4, TG analysis reveals that oxidation begins at 663 K. Maximum weight gains due to oxidation are 11.76% at 1223 K. Final weight gains are 10.00% at 1473 K. A volatile matter, for example  $\text{B}_2\text{O}_3$ , seems to be formed above 1223 K. DTA reveals exothermic peaks at 823 and 927 K. A study of oxidized products by the powder XRD method shows that the products are Rh and  $\text{NdBO}_3$ . The results of TG–DTA are listed in Table 5.

### 3.5 Resistivity and magnetic susceptibility of $\text{NdRh}_3\text{B}_{1.000}$

Fig. 5 shows the temperature dependence of the electric resistivity of  $\text{NdRh}_3\text{B}_{1.000}$ . The sample measured exhibits metallic behavior from room temperature down to 0.5 K. No superconductivity appears at the lowest temperature. Fig. 6 shows the temperature dependence of the magnetization of  $\text{NdRh}_3\text{B}_{1.000}$  in a field  $H = 5000$  Oe. Magnetic susceptibilities for  $\text{NdRh}_3\text{B}_{1.000}$  show Curie-like paramagnetic

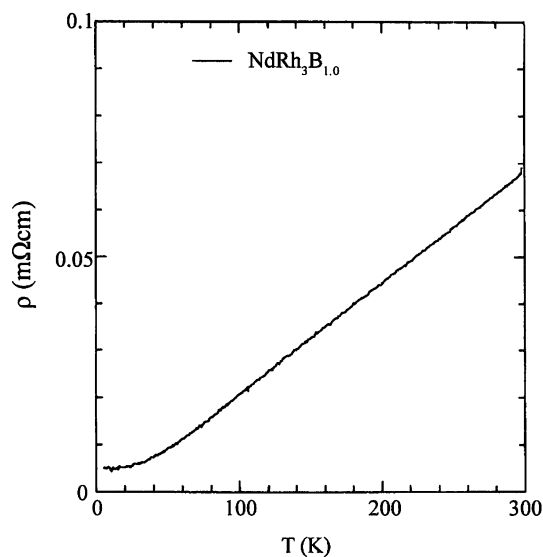
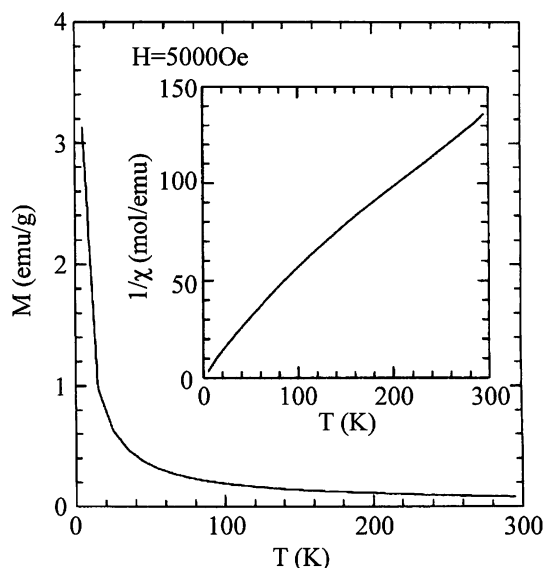
Fig. 4. TG-DTA curves for  $\text{NdRh}_3\text{B}_{1.000}$ .**Table 5** Result of the TG-DTA measurement for the  $\text{NdRh}_3\text{B}_{1.000}$ 

Sample	Oxidation onset (K)	Exotherm maximum (K)	Weight gain (%)	Oxidation products
$\text{NdRh}_3\text{B}_{1.000}$	663 K	823, 927	10.00	Rh + $\text{NdBO}_3$

behavior. No trace of magnetic phase transitions and superconductivity is found down to 0.5 K. The inset shows the linear temperature dependence of the inverse susceptibility. The effective Bohr magneton is calculated to be about 3.5 from the initial slope. This value is close to the theoretical one (3.62) of  $\text{Nd}^{3+}$  ion.

#### 4. Conclusions

1. Polycrystalline samples of  $\text{NdRh}_3\text{B}_x$  have been synthesized by arc melting method [11].
2. The structure of the  $\text{NdRh}_3\text{B}_{1.000}$  is the perovskite-type cubic system (space group  $Pm\bar{3}m$ ) and this phase exists in the range of  $0.706 \leq x \leq 1.000$  (15–20 at.% B). The lattice parameter  $a$  varies linearly from 0.41749(7) nm ( $x=0.706$ ) to 0.42136(6) nm ( $x=1.000$ ).
3. By means of TG-DTA between room temperature and 1473 K, the oxidation of the compound in air starts at 663 K and the final weight gain is 10.00%. The mixed phase of Rh and  $\text{NdBO}_3$  is identified by XRD as a resultant product.

Fig. 5. Temperature dependence of the electric resistivity of  $\text{NdRh}_3\text{B}_{1.000}$ .Fig. 6. Temperature dependence of the magnetization of  $\text{NdRh}_3\text{B}_{1.000}$  in  $H = 5000$  Oe. The inset shows the temperature dependency of inverse susceptibility.

4. The micro-Vickers hardness is  $4.9 \pm 0.05$  GPa for  $\text{NdRh}_3\text{B}_{1.000}$ .
5.  $\text{NdRh}_3\text{B}_{1.000}$  shows a metallic temperature dependence of the resistivity down to 0.5 K.
6. Magnetic susceptibilities for  $\text{NdRh}_3\text{B}_{1.000}$  show Curie-like paramagnetic behavior due to  $\text{Nd}^{3+}$  moment. No trace of magnetic phase transitions and superconductivity is found down to 5 K.

#### Acknowledgements

This work was performed under the inter-university cooperative research program of the ARCMG, IMR, Tohoku University. The authors are grateful to Miss A.

Nomura, Messrs. T. Sugawara, S. Tozawa, Y. Murakami and K. Obara of IMR, Tohoku University, for help during sample preparations and chemical analyses.

### References

- [1] L. D. Woolf, D. C. Johnston, H. B. MacKay, R. W. McCallum, M. B. Maple, J. Low Temp. Phys. 35 (1979) 651.
- [2] For a review, see Superconductivity in ternary compounds II, in: M. B. Maple, O. Fisher (Eds.), Topics in Current Physics, Vol. 34, Springer, Berlin, 1982.
- [3] T. Shishido, I. Higashi, H. Kitazawa, J. Bernhard, H. Takei, T. Fukuda, Boron, borides and related compounds, Jpn. J. Appl. Phys. 10 (Special issue) (1994) 142.
- [4] T. Shishido, K. Kudou, S. Okada, Y. Ye, M. Oku, H. Horiuchi, T. Fukuda, J. Alloys Comp. 280 (1998) 65.
- [5] H. Holleck, J. Less-Common Metals 52 (1977) 167.
- [6] P. Rogl, L. DeLong, J. Less-Common Metals 91 (1983) 97.
- [7] T. Shishido, J. Ye, K. Kudou, S. Okada, K. Obara, T. Sugawara, M. Oku, K. Wagatsuma, H. Horiuchi, T. Fukuda, J. Alloys Comp. 291 (1999) 52.
- [8] T. Shishido, J. Ye, K. Kudou, S. Okada, M. Oku, H. Horiuchi, T. Fukuda, J. Ceram. Soc. Jpn. 108 (7) (2000) 683.
- [9] R. E. Honig, RCA Rev. 23 (1962) 571.
- [10] G. V. Samsonov, I. M. Vinitskii, in: Handbook of Refractory Compounds, IFI/Plenum Press, New York, 1980, p. 303.
- [11] T. Shishido, K. Kudou, S. Okada and K. Nakajima, J. Alloys Comp. 335 (2002) 191.

## ペロブスカイト型 NdRh<sub>3</sub>B のホウ素固溶範囲および性質

岡田 繁<sup>\*1,†</sup>・工藤 邦男<sup>\*2</sup>・飯泉 清賢<sup>\*3</sup>・  
中嶋 一雄<sup>\*4</sup>・宍戸 統悦<sup>\*5</sup>

**和文概要** 多結晶体 NdRh<sub>3</sub>B<sub>x</sub> はアークメルト法で合成した。NdRh<sub>3</sub>B<sub>x</sub> の結晶構造は  $0.706 \leq x \leq 1.000$  (15–20 mol.% B) のホウ素濃度範囲でペロブスカイト型立方晶系 (空間群  $Pm\bar{3}m$ ) である。格子定数  $a$  は  $0.41749(7) \text{ nm}$  ( $x=0.706$ ) から  $0.42136(6) \text{ nm}$  ( $x=1.000$ ) に直線的に変化する。TG 分析では NdRh<sub>3</sub>B<sub>1.000</sub> の酸化開始温度は 663 K である。また、空气中で 1473 K に加熱した時の NdRh<sub>3</sub>B<sub>1.000</sub> の重量増加率は 10.00% で、酸化後の生成物は Rh と NdBO<sub>3</sub> である。NdRh<sub>3</sub>B<sub>1.000</sub> のビッカース微小硬さは  $4.9 \pm 0.05 \text{ GPa}$  である。室温から 0.5 K までの低温度域での NdRh<sub>3</sub>B<sub>1.000</sub> は金属的な振る舞いをしていいる。NdRh<sub>3</sub>B<sub>1.000</sub> の磁化率は Nd<sup>3+</sup> モーメントに依存した漸近キュリーの常磁性温度を示す。その化合物は磁気相転移と超伝導を示さないことが理解できた。